Shang *et al. Applied Biological Chemistry* (2023) 66:22
https://doi.org/10.1186/s13765-023-00779-1

KSABC
The Korean Society for Applied Biological Chemistry

ARTICLE

Open Access

Jasmine tea extract enhances human retinal pigment epithelial cells survival after UVB irradiation

Hu Shang[1], Yaling Guo[1], Liangyu Wu[1*] and Jinke Lin[1*]

Abstract

To examine the protecting effect of jasmine tea extract (JTE) against ultraviolet B (UVB) induced damage on human retinal pigment epithelial (RPE) cells, the RPE cells were subjected to UVB exposure and sequential JTE administration. The cell viability, intracellular reactive oxygen species (ROS), and apoptosis were determined by MTT, 2′,7′-dichlorodihydrofluorescein diacetate and flow cytometer assays, respectively. Further, the cells treated with UVB irradiation and sequential JTE administration were subjected to RNA-sequencing analysis in order to identify genes and pathways involved in the UVB-induced damage and JTE protecting mechanisms. The results showed that JTE effectively attenuated the UVB-induced cell injury by reducing the excessive intracellular ROS generation, and inhibiting the expression of apoptotic genes such as Bax, Caspase-3/9. This finding may offer a promising candidate for the prevention of UVB exposure related eye diseases.

Keywords Jasmine tea extract, Retinal pigment epithelial cells, UVB-irradiation, Oxidative stress, Apoptosis

Introduction

Solar ultraviolet B (UVB) irradiation, with wavelengths from approximately 280 to 320 nm, can penetrate the ozone layer and reach the Earth's surface. A suitable amount of UVB exposure is essential for health benefits, but excessive exposure can lead to inflammation, oxidative stress, DNA mutations, and damage to mitochondria [1–3], leading to the initiation, promotion, and progression of several eye diseases, including cataracts, corneal damage, and age-related macular degeneration (AMD) [4–6]. Retinal pigment epithelial (RPE) cells, located in the outermost layer of the retina, are critical for maintaining neural retina function. Previous studies have shown that continuous UVB exposure can induce several signs of injury in RPE cells, such as decreased cell viability [6], redox imbalances [7], DNA fragmentation [8], and inflammatory signaling [9], all of which are associated with the development of ophthalmic disorders [10].

Jasmine tea is a popular beverage that originated in China and is widely consumed due to its fresh flavor and health benefits, including sedative effects on autonomic nerve activity and antioxidant properties [11–13]. The main bioactive polyphenols in jasmine tea are catechins, including (+)-catechin (C), (−)-epicatechin (EC), (−)-epigallocatechin (EGC), (−)-epicatechin gallate (ECG), (+)-catechin gallate (CG), (+)-gallocatechin gallate (GCG), and (−)-epigallocatechin gallate (EGCG), which have potential anti-photoaging benefits based on their photoprotective and antioxidant activities [14, 15]. Recent studies have shown that catechins can neutralize free radicals induced by UV radiation and reduce damages caused by free radicals [16, 17]. Green tea extract that including catechins can protect against UV irradiation-induced damage in rats by preventing lipid

*Correspondence:
Liangyu Wu
vulay@foxmail.com
Jinke Lin
ljk213@163.com
[1] College of Horticulture, Fujian Agriculture and Forestry University, Fuzhou, China

peroxidation and DNA fragmentation [18]. Catechins have also been shown to alleviate UV-induced protein damage by increasing antioxidative capacity [19]. EGCG, the predominant catechin in teas, promotes human lens epithelial cell survival after UVB exposure by reducing the generation of free radicals and increasing the activity of antioxidant enzymes [20]. As jasmine tea extract is widely available and abundant in the tea industry [21], the utilization of jasmine tea extract (JTE) could be a promising ingredient for developing formulation with antioxidant and photo-protective activities.

To date, there is little direct evidence on the cytoprotective effect of JTE against UVB irradiation. Given the harmful effects of UVB exposure and the potential antioxidant properties of jasmine tea extract, this study aimed to evaluate the protective effect of JTE against UVB-induced injury in RPE cells by measuring cell viability and intracellular ROS levels. In addition, RNA-sequencing and quantitative real-time PCR (qPCR) analyses were also performed to investigate the underlying mechanism of UVB-induced cell damage and the protective effect of JTE. The results of this study could provide new insights into the protective effects of JTE on RPE cells after UVB exposure.

Materials and methods

Cell culture and reagents

The reagents with analytical grade were obtained from Sinopharm Chemical Company (Shanghai, China), and the ultrapure water was supplied by Milli-Q water system (Millipore Company, Bedford, USA). The RPE cells (ARPE-19, American Type Culture Collection, Manassas, VA, USA) were cultured in Dulbecco's modified Eagle's medium (Gibco, Rockville, MD, USA) with 10% fetal bovine serum (Gibco, Rockville, MD, USA) at 37 ℃, 5% CO_2 and 100% relative humidity. The jasmine tea sample was purchased from Chunlun Ltd. Co. (Fuzhou, China), and the preparation of JTE was as follows: the dry tea sample was ground into powder and filtered through a 40-mesh sieve. Then, one gram of the tea powder was mixed with 50 mL of ultrapure water in a flask and incubated in a water-bath at 95 ℃ for 30 min. The resulting JTE supernatant was filtered using a 0.22 μm membrane and subjected to HPLC analysis. The major components of JTE are listed in Table 1.

UVB irradiation

The UVB irradiation was conducted by using UVB lamps (FLS Inc., Foushan, Guangdong, China). These lamps emit wavelengths with the range of 290–320 nm and the intensity of UVB was examined by a UV-meter (UV-340, Optical instrument factory of Beijing Normal University, Beijing, China). RPE cells were seeded onto a 96-well plate with 1×10^5 cells per well and allowed to reach 70–80% confluence. Prior to UVB irradiation, the culture medium was replaced with serum-free Dulbecco's modified Eagle's medium. The cells in UVB group were exposed to irradiation with a dose of 100 mJ/cm^2. For UVB-JTE sequential treated group, the cells were initially subjected to 100 mJ/cm^2 UVB irradiation, then the JTE was immediately administrated into each well after UVB exposure (JTE: culture medium = 1:9, V/V). Subsequently, the cells in UVB and UVB-JTE groups were incubated at 37 ℃ for 30, 60, 120, 240 and 480 min. The cells treated without irradiated nor JTE were set as normal control.

MTT assay

The cell viability in different groups was determined by MTT assay. In brief, 20 μL of methyl thiazolyl tetrazolium solution (0.5 mg/mL) was added to each well of 96-well plate, and the plates were incubated at 37 °C for 4 h. The solution was pipetted out, and 200 μL dimethyl sulfoxide was added, then shaken at 100 rpm/min for 5 min. The formazan dye formation was measured at 540 nm using an ELISA reader (Thermo Fisher Scientific Inc., Waltham, MA, USA). The results were expressed as a percentage of viability with respect to the normal control.

Detection of intracellular reactive oxygen species (ROS)

The cells were seeded onto a culture dish (ϕ 3.5 cm) with a diameter of 3.5 cm at a density of 1×10^5 cells/mL.. After reaching 70–80% confluence, the cells on each dish were firstly treated with 10 μM of 2′,7′-dichlorodihydrofluorescein diacetate (DCF-DA), then incubated at 37 ℃ for 30 min. Subsequently the cells were washed three times with PBS. The DCF-DA loaded cells were subjected to the UVB-irradiation or UVB-JTE sequential treatment, then the fluorescence in different groups was observed using a laser confocal scanning microscope (FV1200, Olympus Corporation, Tokyo, Japan) with excitation wavelength at 488 nm and

Table 1 The concentration of catechins and caffeine in the jasmine tea extract* (mg/L)

GA	CAF	C	EC	EGC	ECG	CG	GCG	EGCG
62.47 ± 1.03	641.48 ± 20.14	396.77 ± 7.98	352.99 ± 12.58	61.57 ± 5.96	228.22 ± 18.26	63.57 ± 3.02	106.85 ± 7.56	870.97 ± 19.87

* *GA* gallic acid, *CAF* caffine, *C* (+)-catechin, *EC* (−)-epicatechin, *EGC* (−)-epigallocatechin, *ECG* (−)-epicatechin gallate, *CG* (+)-catechin gallate, *GCG* (+)-gallocatechin gallate, *EGCG* (−)-epigallocatechin gallate

emission wavelength at 525 nm. For quantitated test, the cells were seeded on 96-well plates, then followed by the same protocol as above, the fluorescence intensity of ROS was determined by a fluorescence ELISA reader (Infinite M200 pro, Tecan Corporation, Mannedorf, Switzerland).

The apoptosis determination

The RPE cells were seeded on a culture dish with a diameter of 10 cm at a density of 1×10^5 cells/mL. When the cells reached 70–80% confluence, they were treated with either UVB irradiation or UVB-JTE sequential treatments as described earlier. Then the cells in different groups were respectively collected using the cell scrapers, and transferred into 1.5 mL centrifuge tube. The cells were rinsed by PBS for three times, then centrifuged at 2000 rpm for 5 min, followed by adding 450 μL binding buffer, 5 μL 7-amino-actinomycin D (7-AAD) and 1 μL Annexin V-PE (Keygen Biotechnonology, Nanjing, China), incubated at 37 ℃ for 15 min. Then the fluorescence of cells apoptosis was determined on a flow cytometer (EasyCyte, Merk Group, Darmstadt, Germany).

Analysis of RNA-sequencing

For each sample, three independent biological replicates were used and cells were collected separately for RNA sequencing analysis. RNA isolation was performed according to the protocol of an RNA isolation kit from Bioer Technology (Hangzhou, China), and the RNA sequencing was carried out by Novogene Bioinformatics Technology Co., Ltd (Beijing, China) using an Illumina HiSeq2500 platform and the standard Illumina RNA-Sequencing protocol. RNA integrity was assessed on 1% agarose gels, and RNA concentration was estimated using an Agilent 2100 Bioanalyzer (Agilent Technologies, Inc., Santa Clara, CA, USA). Downstream analysis of the RNA sequencing data was performed using a combination of programs including Bowtie2, Tophat2, HTseq and Cufflink. The edge R package was used to identify differentially expressed genes (DEGs) with the criterion of fold change > 2 ($P < 0.05$). Enrichment analysis on the DEGs using the Kyoto Encyclopedia of Genes & Genomes (KEGG) and gene ontology (GO) was implemented by GOseq R package and KOBAS.

Quantitative real-time PCR (qPCR) analysis

The PrimeScript Reagent Kit (TaKaRa, Dalian, China) was applied to the synthesis of first-strand cDNA from 1 μg of total RNA. The gene-specific primers were designed on Primer 3 software (Table 2), and the gene of reduced glyceraldehyde-phosphate dehydrogenase (GAPDH) was used as the endogenous control to normalize expression between different samples. The PCR reactions were run on a Bio-Rad CFX96 platform using the following program: 95 °C for 15 s and 40 cycles at 95 °C for 10 s, annealing at 60 °C for 30 s. Each reaction was performed in triplicate, in which the average threshold cycle was calculated to estimate the relative gene expression levels using the $2^{-\Delta\Delta Ct}$ method [22].

Table 2 The primer sequences for qRT-PCR

Gene		Primer (5′→ 3′)
GAPDH	F	GACCATAGCAGGGACAAGGT
	R	TTCCTCCATCCCTGTTGTCC
p53	F	CTGGCATTTGCACCTACCTC
	R	TAACCAGCTGCCCAACTGTA
Bax	F	CTTCTGGAGCAGGTCACAGT
	R	AAGGTCACAGTGAGGTCAGG
ERK2	F	ACCAACCTCTCGTACATCGG
	R	TAGGTCTGGTGCTCAAAGGG
COX5B	F	GAGGTGGTGTTCCCACTGAT
	R	TTTGCAGCCAGCATGATCTC
Caspase-9	F	GGGAGTCAGGCTCTTCCTTT
	R	CTGAGAACCTCTGGTTTGCG
Caspase-3	F	TCGGTCTGGTACAGATGTCG
	R	CTTCACCATGGCTCAGAAGC
Bcl-2	F	GACTTCGCCGAGATGTCCAG
	R	CCACCGAACTCAAAGAAGGC
Bcl-XL	F	CGTGGAAAGCGTAGACAAGG
	R	GCTGCTGCATTGTTCCCATA
SOD1	F	GGAGACTTGGGCAATGTGAC
	R	GACTTCCAGCGTTTCCTGTC
GPx1	F	CCCTCTCTTCGCCTTCCTG
	R	GCTCGATGTCAATGGTCTGG

Statistical analysis

All the experiments were carried out in triplicates and the data was analyzed by one-way analysis of variance using the least significant difference as a multiple range test on Origin 8.0 software (OriginLab Inc., Northampton, MA, USA).

Results

JTE alleviates UVB-induced cell injury

The results of methyl thiazolyl tetrazolium (MTT) assay showed that the viability of UVB-exposed cells decreased from 51 to 8% within 480 min, indicating continuous injury after UVB irradiation (Fig. 1A). In contrast, the cell viability in the UVB-JTE group (UVB-JTE) was 78% after 30 min JTE treatment, and then decreased to 17% within 480 min, which was significantly higher than that of UVB group (Fig. 1A). These findings suggest that JTE treatment attenuated the persistent cytotoxicity in UVB-exposed RPE cells. Additionally, the cell apoptosis within 120 min after UVB exposure was determined using flow

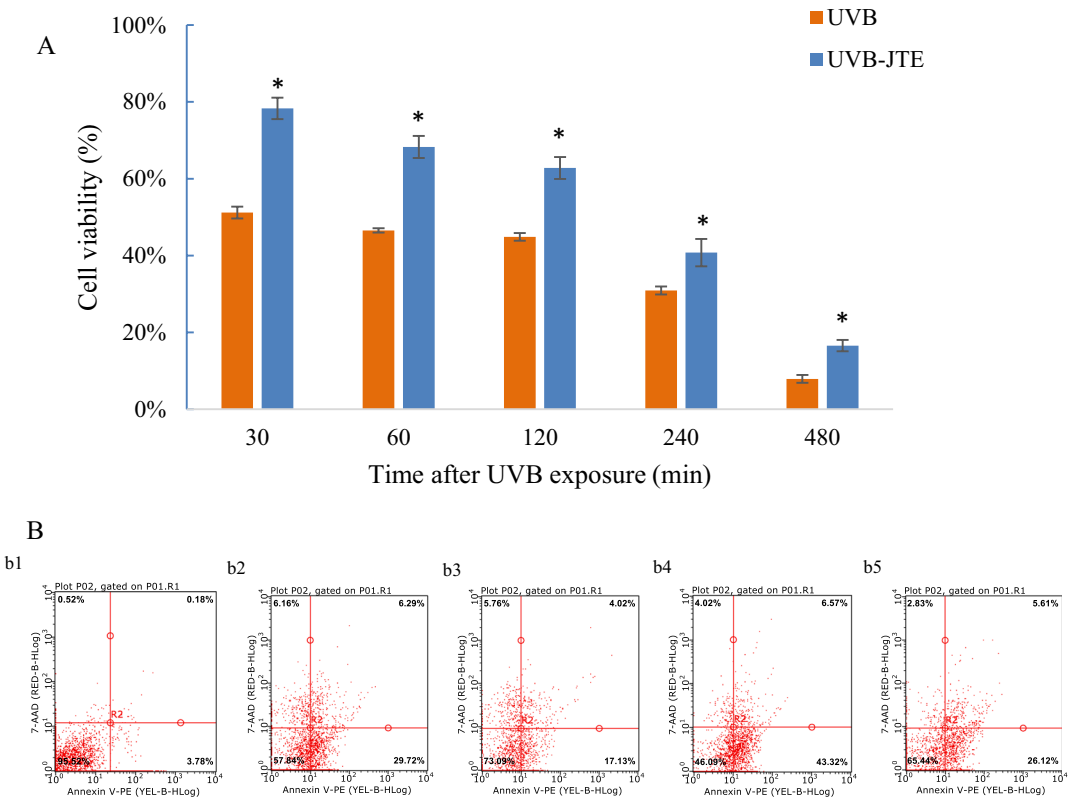

Fig.1 The cell viability (**A**) and flow cytometer determination (**B**) of different treated cells. **A** RPE cells exposed to UVB irradiation then treated with or without JTE treatment for 30, 60, 120, 240, 480 min. The viability of UVB and UVB-JTE treated cells was calculated by comparing with normal cells. Statistical comparisons were performed between groups treated with same time ($P < 0.05$). **B** The flow cytometer analysis of the apoptosis of various treated RPE cells. b1: normal cell; b2: 30 min after UVB irradiation; b3: 30 min after UVB irradiation and sequential JTE treated; b4: 120 min after UVB irradiation; b5: 120 min after UVB irradiation and sequential JTE treatment

cytometer assay. The normal, early apoptotic, later apoptotic and necrotic cells were respectively distributed on lower left, lower right, upper right and upper left quadrants of two-dimensional scatter diagram (Fig. 1B). The result of flow cytometer detection showed that the proportion of apoptotic cells in UVB group clearly increased, reaching 36.01% and 49.89% at 30 and 120 min after UVB-exposure respectively, compared to 3.96% in normal cells group (NC) as showed in Fig. 1B. In contrast, the apoptotic cells in UVB-JTE group accounted for 21.15% and 31.73% at 30 and 120 min after UVB irradiation (Fig. 1B), suggesting that JTE treatment alleviated UVB-induced apoptosis, which is consistent with the results of the MTT assay in this study (Fig. 1A).

JTE prevented UVB-induced excessive ROS generation in RPE cells

The 2′,7′-dichlorodihydrofluorescein diacetate (DCF-DA) stained intracellular ROS levels in different groups were presented in Fig. 2A. The fluorescence images showed that the UVB irradiation increased the intracellular ROS level in cells after exposure, and the gradually increased ROS intensity was observed within 30–120 min after UVB irradiation (Fig. 2A, a5-a6, a11-a12). Additionally, the cells after exposure became round or oval, with some irregular wrinkle on the surface (Fig. 2A, a4, a10), in contrast to the spindle-sharped cells in NC group (Fig. 2A, a1). The JTE treatment reduced the UVB-triggered intracellular ROS increase in cells, the amount of DCF-DA

(See figure on next page.)

Fig. 2 Effect of UVB irradiation and jasmine tea extract on the generation of intracellular ROS in RPE cells. **A** The laser confocal microscopy after DCF-DA staining on reactive oxygen species (green spots) in optical view (column 1), fluorescence view (column 2) and merged view (column 3) respectively; a1-a3: normal cell; a4-a6: 30 min after UVB exposure; a7-a9: 30 min after UVB exposure with sequential JTE treatment; a10-a12: 120 min after UVB exposure; a13-a15: 120 min after UVB exposure with sequential JTE treatment. **B** DCF-DA fluorescence intensity after various treatments, different letters represent significant difference ($P < 0.05$)

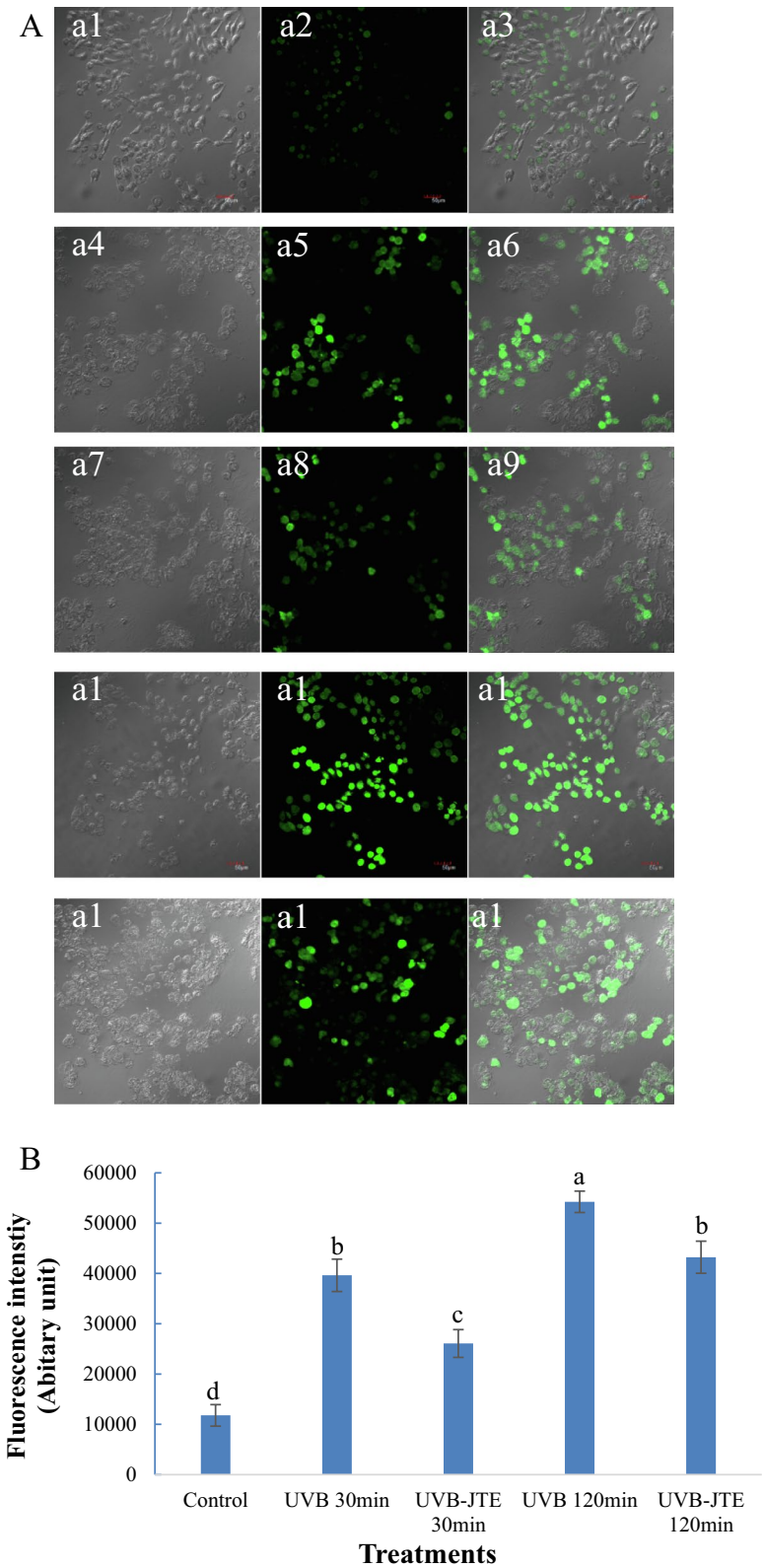

Fig. 2 (See legend on previous page.)

fluorescence intensity was clearly decreased comparing to those of UVB group (Fig. 2A, a8-a9, a14-a15), and most of the cells were similar to normal morphology after JTE-treatment (Fig. 2A, a7, a13). The quantitative determination of intracellular ROS levels in different groups revealed that UVB irradiation significantly promoted the intracellular ROS level in RPE cells comparing to that of normal cells, and the subsequent JTE treatment obviously retarded the excessive ROS generation over 120 min after UVB-exposure (Fig. 2B), demonstrating a persistent intracellular ROS scavenging capacity.

The result of RNA-sequencing

In order to further investigate UVB-induced damage and JTE protecting mechanism in RPE cells, the RNA-sequencing analysis was performed using an Illumina High-Seq 2500 platforms. The sequencing data were blasted against human genome, the statistics on raw and filtered sequencing data were shown in Table 3. The genes with an average value of fragments per kilobase million (FPKM) higher than 1.0 were further analyzed. As a result, the RNA-seq libraries of normal cells, UVB and UVB-JTE groups obtained approximately 46.3–64.0 million clean reads, over 85% clean reads were matched to the reference genome, a total of 48,163 genes were identified and applied to the analysis on the dynamic changes of genes expression among different groups (Additional file 1: Table S1 The genes identified in RNA-sequencing).

The principal component analysis (PCA) of identified genes showed that the cell samples were clustered and discriminated from each other according to the RNA-seq profiles (Fig. 3A). The first two components, PC1 and PC2, accounted for nearly 75.8% of the variance, meeting the general requirements of cumulative percent variance > 70 − 85% for PCA analysis [23]. Figure 3B showed the amount of differently regulated genes (DEGs) in different paired-comparisons. The most abundant DEGs were observed in the comparison of UVB-JTE/Control, with 3941 up-regulated and 3481 down-regulated DEGs, followed by the UVB/Control (3042 up-regulated and 2343 down-regulated DEGs), the comparison of UVB-JTE/UVB had the lowest number of DEGs (1587 up-regulated and 908 down-regulated DEGs, Fig. 3B, Additional file 2: Table S2 The DEGs identified in different comparisons), suggesting the UVB-irradiation and

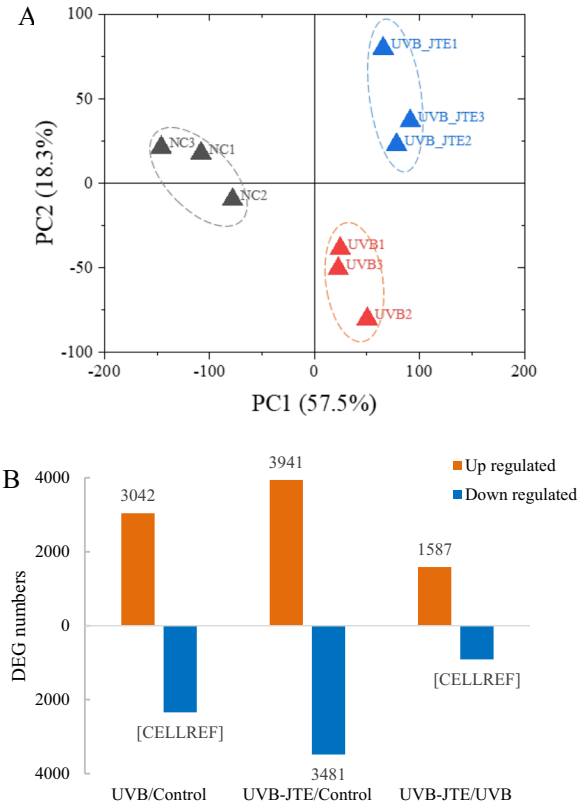

Fig. 3 PCA analysis of identified genes (**A**) and The DEG numbers (**B**) in different groups

Table 3 The statistics of RNA-sequencing results*

12	Raw reads	Clean reads	Q20 (%)	GC content (%)	The reads mapped to genome/total clean reads (%)
NC_1	67310,952	64041634	97.77	51.04	89.36
NC_2	60791928	57774348	97.8	52.55	88.85
NC_3	57845508	54946150	97.75	51.18	88.56
UVB_1	52316338	49320502	97.48	53.57	85.94
UVB_2	59554908	46346178	99.33	55.85	88.35
UVB_3	52612196	49410512	97.59	54.56	85.14
UVB-JTE_1	53404866	50511122	97.65	52.57	87.13
UVB-JTE_2	68128904	61173526	98.36	54.66	86.81
UVB-JTE_3	61464724	57914074	97.61	54.55	85.60

the subsequent JTE treatment triggered the dynamic changes of gene expression compared with that of normal cells. The qPCR analysis of the ten genes related to cell apoptosis pathway was used to validate the transcriptomic profile, the result showed the qPCR dataset were in a general agreement with the transcriptomic profile, with R^2 being 0.91 (Fig. 4), indicating that the transcriptomic data were able to reflect the transcript abundances in this work.

Functional enrichment analyses of DEGs

Kyoto Encyclopedia of Genes & Genomes (KEGG) and gene ontology (GO) GO categorization were used to identified the DEGs annotated with functions. Three comparison pairs were categorized into the GO terms including biological process, molecular function, and cellular component (Fig. 5). The pair of UVB/Control had the most enriched DEGs in "binding" of molecular function and "cellular process" of biological process categories, respectively (Fig. 5A), the enrichment with similar magnitude was also observed in the comparison of UVB-JTE/Control (Fig. 5B), which is consistent with the aforementioned results in DEG amounts of different comparisons (Fig. 3B).

Figure 6 showed the top ten enriched pathways in different paired-comparisons based on KEGG analysis of DEGs. The most DEGs enriched pathway in UVB/Control and UVB-JTE/Control was "Ribosome", while the counterpart in UVB-JTE/UVB was "Lysosome" (Fig. 6). There were several shared pathways appeared in both of the UVB/Control and UVB-JTE/Control comparisons, including "Parkinson's disease", "Huntington's disease", "Alzheimer's disease", "Non-alcoholic fatty liver disease (NAFLD)", "Oxidative phosphorylation" (Fig. 6A, B), suggesting a great change in genes associated with these diseases were involved in the injury of UVB-exposed RPE cells and the subsequent JTE treatment. Together with the similar changes in the GO and KEGG analyses on different treated cells, it is postulated that the same genes or pathways were involved in the UVB-mediated cytotoxicity and the JTE cyto-protection effect in this study.

The genes involved in the cytoprotective mechanism of JTE

To further investigate the genes involved in the cytoprotective mechanism of JTE, the 48,163 genes identified in RNA-seq dataset were filtered with the criterial of the average FPKM value higher than 1.0. As a result, a total of 13,355 genes (Additional file 3: Table S3 The filtered genes) in all samples were obtained and hierarchically clustered to provide subgrouping information using Short-Time-series Expression Miner and R package. Roughly, the cell samples from different groups were hierarchically categorized, and the genes in different groups could be classified into four subgroups according to their expression profiles (Fig. 7A). Notably, the genes enriched in subcluster2 were potentially involved in the cell damage and JTE protecting mechanism, since the expression pattern showed a resemblance with the results of cell viability and intracellular ROS level. Further, the KEGG pathway analysis on the genes enriched in subcluster2 was performed, the result demonstrated the genes enriched in subcluster2 were predominantly assigned to 15 pathways with the adjusted *P*-value lower than 0.05 (Fig. 7B). Then the genes associated with these

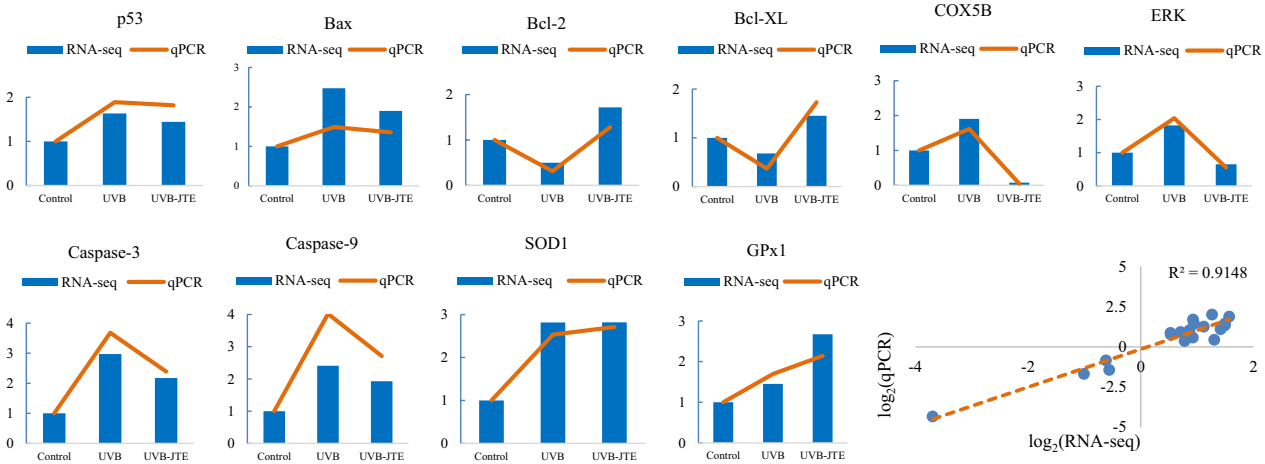

Fig. 4 The genes associated with apoptosis pathway were selected for the quantitative real-time PCR (qPCR) analysis. The genes expressions of UVB and UVB-JTE were normalized to normal control, and GAPDH gene was chosen as the endogenous control for qPCR. p53: tumor protein p53; Bax: apoptosis regulator Bax; Bcl-2: apoptosis regulator Bcl-2; Bcl-XL: apoptosis regulator Bcl-XL; COX5B: Cytochrome c oxidase subunit 5B; ERK: mitogen-activated protein kinase 1/3; SOD1: superoxide dismutase; GPx1: glutathione peroxidase

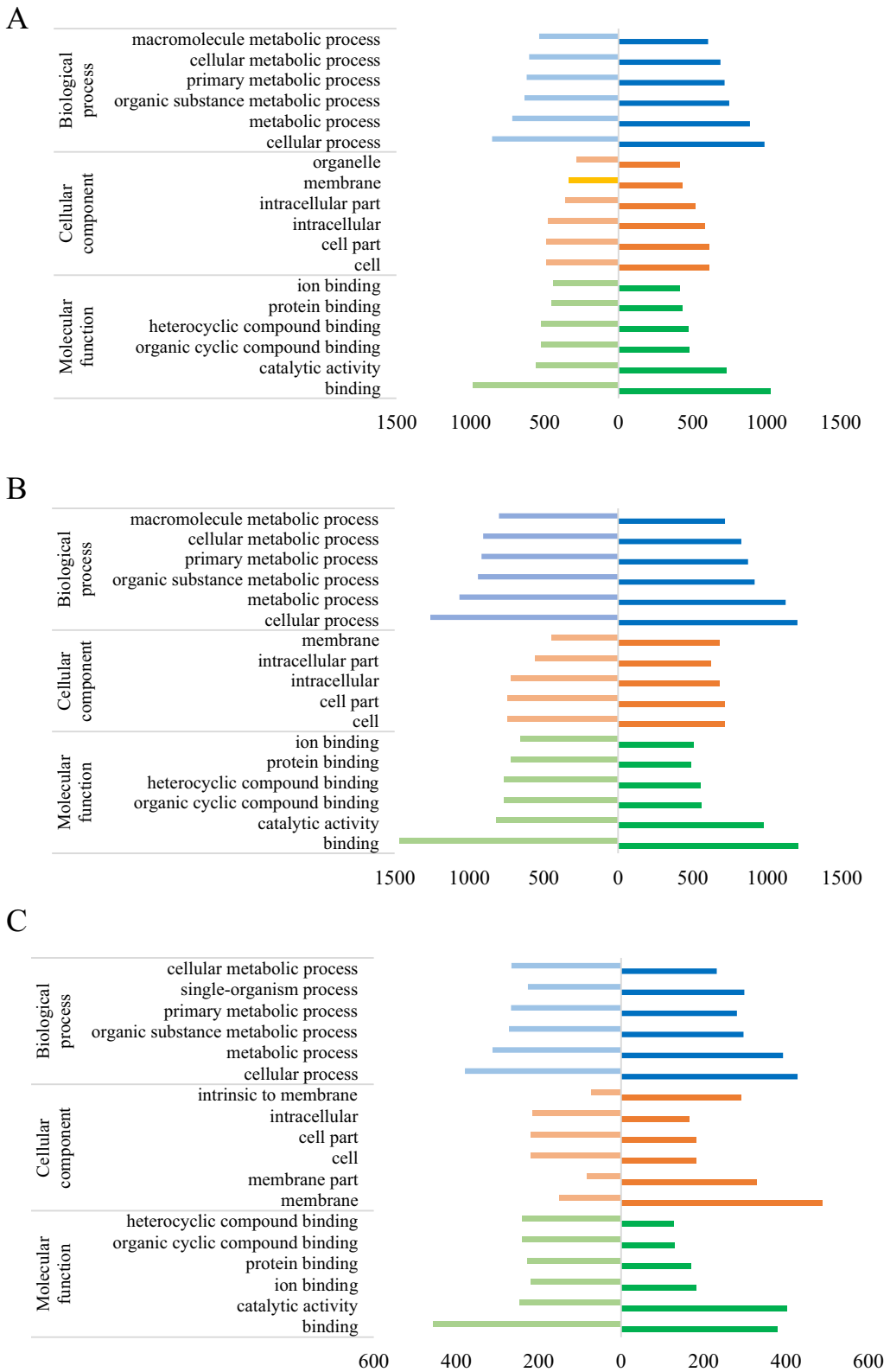

Fig. 5 GO-based functional enrichment analysis of DEGs in (**A**) UVB/Control, (**B**) UVB-JTE/Control, and (**C**) UVB-JTE/UVB, respectively. Bar charts indicate the number of DEGs that were up- (right of X-axis) and down-regulated (left of X-axis), annotated with functions (Y-axis)

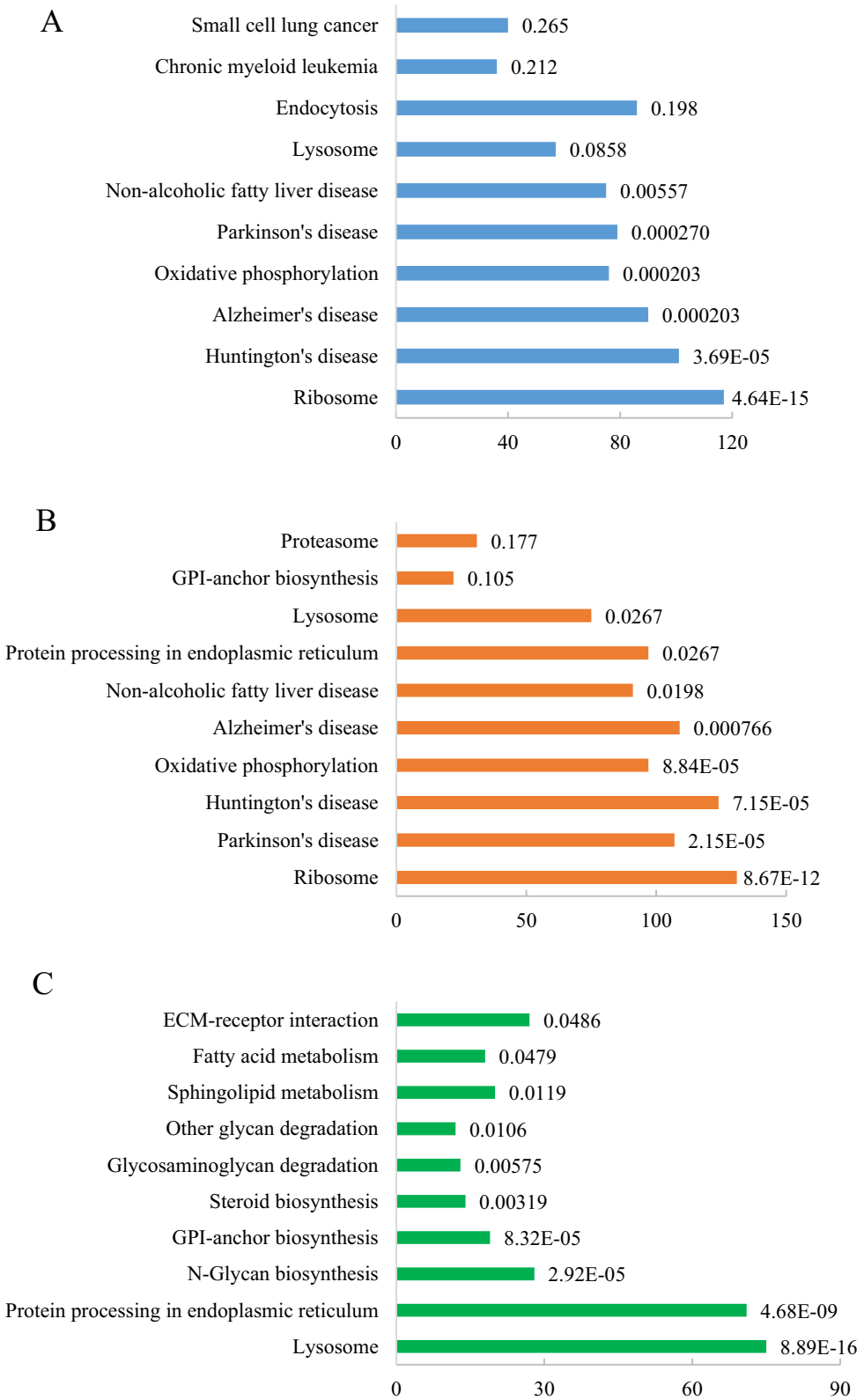

Fig. 6 The top 10 pathways enriched in KEGG-based analysis of DEGs in (**A**) UVB/Control, (**B**) UVB-JTE/Control, and (**C**) UVB-JTE/UVB, respectively. The adjusted *P*-values are annotated at the right of the bar charts

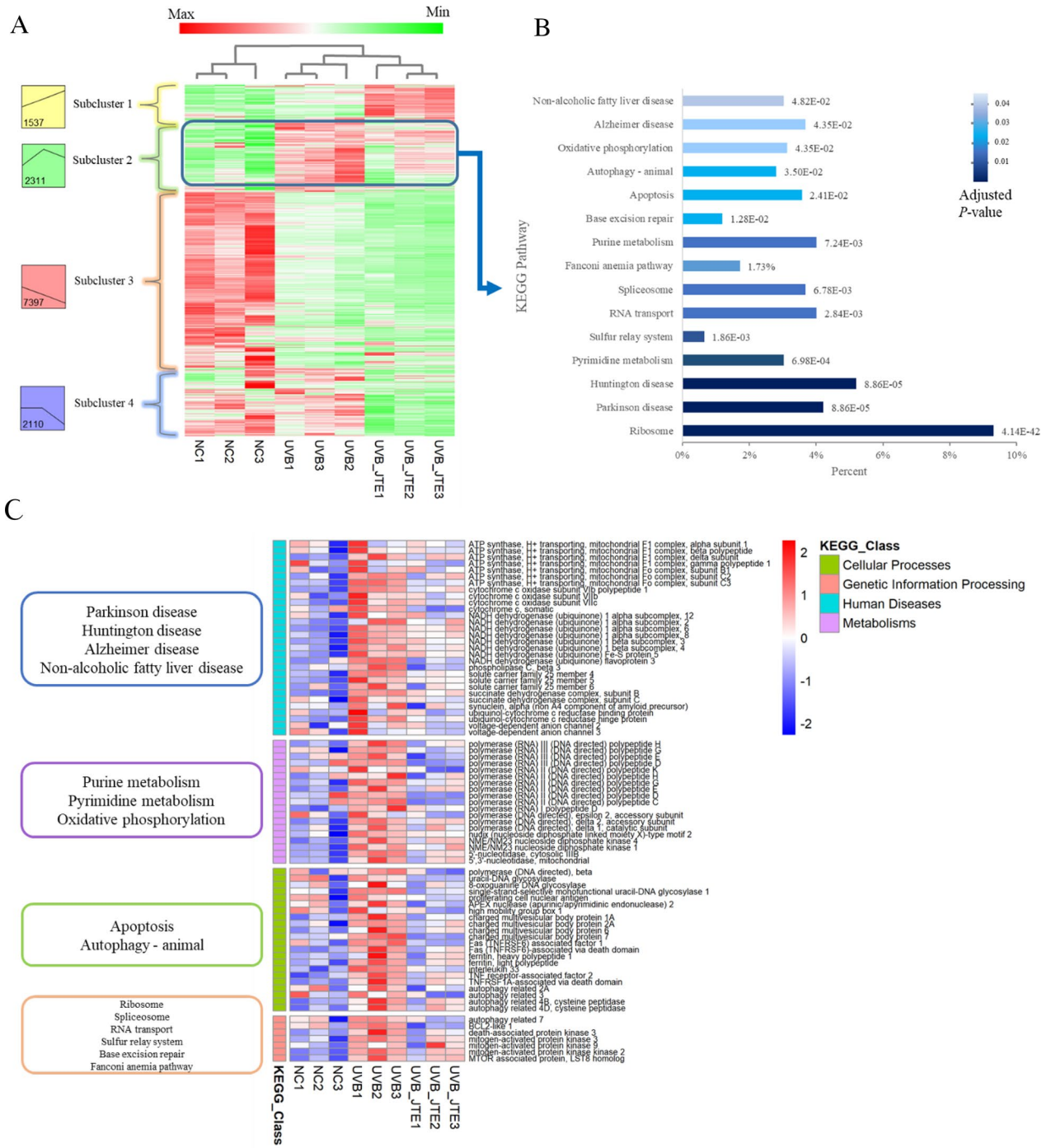

Fig. 7 The RNA-sequencing analysis on RPE cells. **A** Heatmap of 13,355 filtered genes expression and hierarchical clustering. Each cell represents a value of $\log_2$-normalized expression of gene. The boxes at the left show the number of genes with similar expression trend in one cluster. **B** The KEGG-pathway based enrichment analysis of genes expression, with adjusted *P*-value annotated at the right of the bar. **C** Heatmap of 78 genes involved in UVB-mediated cell damage and JET protecting mechanism

15 pathways were subjected to the co-expression analysis using R package, and the expression pattern of shared genes in the same KEGG class were presented in the heatmap, in which a total of 78 genes were obtained and clustered (Fig. 7C). The most abundant KEGG category is Human Disease (30 genes), followed by

Cellular Processed (22 genes), Metabolisms (19 genes), and Genetic Information Processing (7 genes). The "Human Disease" clade enriched the Parkinson disease, Huntington disease and Alzheimer disease, showing an accordance with the result of KEGG analysis on DEGs (Fig. 6A, B). The genes involved in the pathway analysis were mainly associated with oxidative stress, including ATP synthase, cytochrome c oxidase, NADH dehydrogenase, and succinate dehydrogenase, suggesting that oxidative stress played a major part in the injury of UVB-exposed RPE cells and JTE protection effect (Fig. 8)

Discussion

The major features of the RPE cells are their tight junctions between neighboring cells which functions to control the absorption of light irradiation and transport of metabolites between photoreceptors and choroidal capillaries [7]. The depletion of the ozone layer contributes to the greater fluxes of UVB on the earth's surface, resulting in the increase of oxidative stress, altered apoptosis, as well as degeneration of RPE cells, which are responsible for the pathogenesis of AMD [10, 24]. The pretreatment of green tea extract on fibroblast cells could attenuate the UVB light-induced oxidative stress, increased the cell viability by 71% [25]. Our previous study also indicated that green tea extract could increase the survival of UVB stressed RPE cells via inhibiting the dysfunction in organelle [26]. As the major component of tea extra, EGCG protected against UVB-induced human lens epithelial cell apoptosis by inhibiting the H_2O_2 generation [20]. In the present study, the jasmine tea extract effectively enhanced RPE cell survival after UVB exposure, and suppressed the UVB-induced apoptosis of RPE cells (Fig. 1), which is agreed with the previous studies.

The excessive UVB causes harm to living organisms mainly through injuring proteins or DNA, as well as triggering oxidative stress via the production of ROS, resulting in the apoptosis of RPE cells and retinal damage [27, 28]. It has been reported that ROS level was elevated as early as 30 min after UVB-exposure, and the apoptosis of RPE cell arrived at 30.76% within 24 h, suggesting a continuous damage to the cells [29]. The tea extract, with massive catechins, has the great efficiency in antioxidant capacity and UV protection, which could trap superfluous ROS caused by UV irradiation, arresting the persistent injury even after exposure [19, 29]. In the present study, the ROS level in UVB-treated RPE cells was dramatically higher than those in normal cells, while the ROS accumulation was reduced after sequential JTE administration (Fig. 2), this ROS scavenging effect mainly derived from the chelating ability of hydroxyl group of catechins in tea extract [30]. In addition, the results of previous studies indicated that the combination of several catechin monomers showed a synergistic effect in antioxidant activity, which suppressed H_2O_2-induced intracellular ROS production in RPE cells [31–33]. In this study, the cathine compounds in jasmine tea extract were

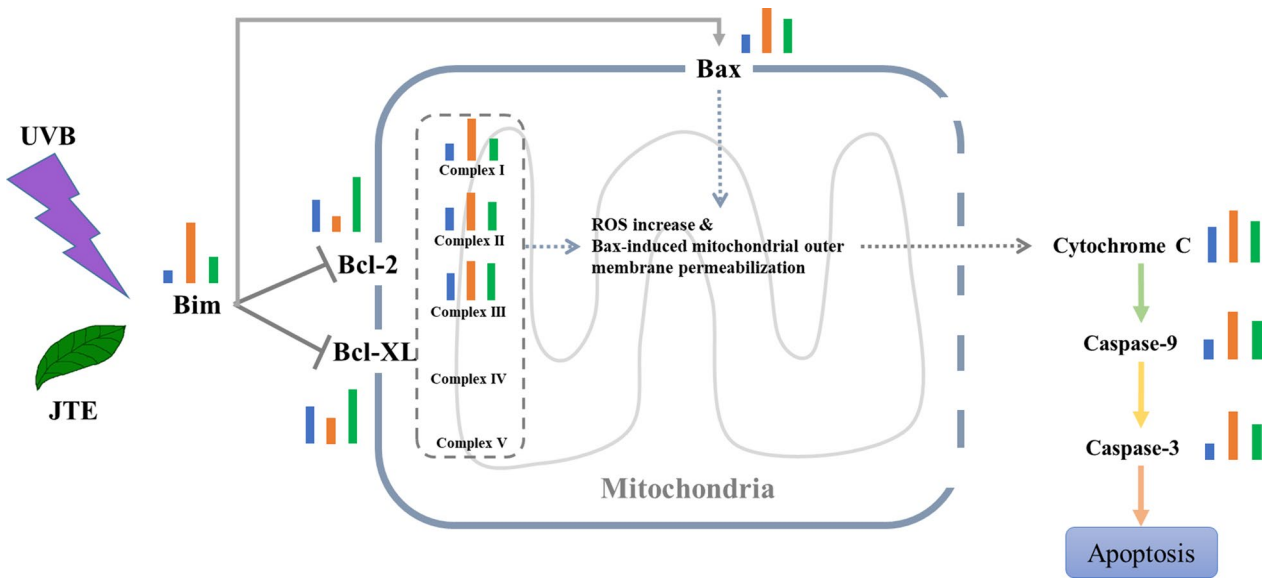

Fig. 8 The schematic of photoprotective mechanism of JTE. Redrawn from the KEGG Apoptosis Reference Pathway (https://www.kegg.jp/kegg-bin/show_pathway?map04210). The bar plots represent the gene expression in normal control, UVB and UVB-JTE samples respectively from left to right. Bim: Bcl-2-like protein 11; Complex I: NADH-ubiquinone oxidoreductase; Complex II: succinate dehydrogenase; Complex III: ubiquinol-cytochrome c reductase

composed of EGCG, ECG, EGC etc., these components displayed strong inhibition of ROS after UVB exposure, and the antioxidant activity of these catechins are not only highly dependent on their structure but also on the synergistic effect.

In age related disorders such as Alzheimer's disease (AD), Huntington's disease (HD), and Parkinson's disease (PD), mitochondria may play an important role, as mitochondria supplies ATP to the cell by oxidative phosphorylation, synthesizes key molecules and responds to oxidative stress as well as in apoptosis [34]. The pathway enrichment analysis in this study also showed that the genes associated with AD, HD, PD and apoptosis were significantly expressed in UVB and UVB-JTE cells respectively (Fig. 7C), implying that oxidative stress induced mitochondrial dysfunction could be a mechanism underlying the UVB-triggered RPE cells apoptosis. The mitochondrial electron transport chain is one of the important main sources of ATP in the mammalian cell and is thus essential for life. The largest amounts of ROS are produced in mitochondria by the transfer of unpaired electrons from semi-ubiquinone or from semi-reduced flavins of complex I (NADH dehydrogenase), complex II (succinate dehydrogenase), and complex III (ubiquinol-cytochrome c reductase) to $\cdot O_2^-$, and the electron transport in complexes I, III which is used by the ATP synthase (complex V) to synthesize ATP from ADP and phosphate, then increased ROS level in mitochondria can ultimately lead to apoptosis [35]. The central event in the intrinsic apoptotic pathway is the mitochondrial outer membrane permeabilization, which is regulated by the pro-apoptotic proteins (Bax, Bak) and anti-apoptotic proteins (Bcl-2, Bcl-XL) [36]. Bax plays a key role in the release of mitochondrial intramembrane space proteins, such as cytochrome C, to aggravate mitochondrial outer membrane permeabilization, resulting in the activation of Caspase-induced apoptosis [37]. As we showed in Fig. 8, the gene expression of NADH dehydrogenase, succinate dehydrogenase and cytochrome c reductase remarkably enhanced after UVB-exposure in this study, in contrast to those in normal cells, indicating excessive oxidative stress were presented in the cells after UVB-exposure, potentially triggering the apoptosis process. However, the JTE treatment effectively reversed the expression levels of Bax and Bcl-2 in RPE cells. This result is in line with the previous research, in which UVB exposure induced apoptosis of lens epithelial cells by boosting the levels of Bax, while EGCG inhibited the apoptosis by regulating the Bcl-2/Bax ratio [20].

The levels of cytochrome c in the cytoplasm are a signal of mitochondrial injury, which results in the cell apoptosis. The catechins have been reported to suppress the release of cytochrome c from the mitochondria into the cytoplasm, contributing to the inhibition of mitochondria-mediated apoptosis [38]. After the release from the mitochondria into the cytoplasm, the cytochrome c combined with Apaf-1 and pro-Caspase-9 to form the apoptotic body, the Caspase-9 is activated and then further cleaved downstream effector Caspases, including Caspases-3, leading to the execution of apoptosis [39]. The catechins, were able to reduce the cell viability loss and apoptosis by eliminating ROS overproduction and overexpression of cleaved-Caspase 3, Caspase 9, cytochrome c [40, 41]. In the present study, the JTE consisted of catechins efficiently protected UVB-stressed RPE cells from apoptosis by limiting the expression of cytochrome c, Caspase-9 and Caspase-3, indicating that JTE could block the mitochondria-mediated cell apoptosis pathway.

The results in this study demonstrated JTE protected RPE cells from the UVB-caused persistent damage at post-irradiation stage by reducing the intracellular ROS level and regulating the apoptotic signaling pathway, in agreement with the protective effects of polyphenols in plant extract against UV-mediated oxidative damage [42–44]. These results exhibit the JTE could be a feasible compound in UV-protective or after-sun injury healing preparations to prevent UVB-caused eye disease occurrence. The present study only determined the expression of genes, such as Bcl-2, Bax, cytochrome c, Caspase-9 and Caspase-3 in vitro, however, experiments in vivo with humans are needed to validate the effects of JTE protecting against UVB irradiation and inhibiting the pathogenesis of eye diseases with desirable clinical physiological properties.

The present study investigated the protective effect of jasmine tea extract on RPE cells after UVB exposure. The results indicated that UVB irradiation induced apoptosis in RPE cells through intracellular ROS stress. However, JTE was able to scavenge the excess ROS, alleviate continuous cell damage after exposure, and significantly increase cell viability. Furthermore, JTE efficiently prevented UVB-induced apoptosis via the mitochondrial signaling pathway by regulating the expression of Bax, Bcl-2, cytochrome c, Caspase-9, and Caspase-3. These findings suggest that JTE may play a protective role and have potential applications in preventing UVB-caused eye diseases.

Supplementary Information

The online version contains supplementary material available at https://doi.org/10.1186/s13765-023-00779-1.

Additional file 1: Table S1. The genes identified in RNAsequencing.

Additional file 2: Table S2. The DEGs identified in different comparisons.

Additional file 3: Table S3. The filtered genes.

Acknowledgements
Not applicable.

Author contributions
Methodology and investigation HS; project administration and writing—review and editing, YS; project administration and funding acquisition, YG; investigation and analysis, LW. All authors read and approved the final manuscript.

Funding
This study was supported by the Construction Project for Technological Innovation and Service System of Tea IndustryChain (K1520005A07), the Jasmine Industry Promoting Project of Fuzhou (K15150510), China Agriculture Research System of MOF and MARA (CARS-19), and Characteristic Quality Study on Laocong Shuixian Teas (KH190365A).

Availability of data and materials
The raw data of RNA-sequencing has been deposited to the sequence read archive database of National Center for Biotechnology Information (NCBI) under the accession number of SRP126644.

Declarations

Competing interests
The authors declare that there is no competing interest in this study.

Received: 5 January 2023 Accepted: 27 March 2023
Published online: 18 April 2023

References

1. Fitsiou E et al (2021) Cellular senescence and the senescenceassociated secretory phenotype as drivers of skin photoaging. J Investig Dermatol 141(4):1119–1126
2. Cadet J, Douki T (2018) Formation of UV-induced DNA damage contributing to skin cancer development. Photochem Photobiol Sci 17(12):1816–1841
3. Schuch AP et al (2017) Sunlight damage to cellular DNA: Focus on oxidatively generated lesions. Free Radical Biol Med 107:110–124
4. Haag R, Sieber N, Hessling M (2021) Cataract development by exposure to ultraviolet and blue visible light in porcine lenses. Medicina-Lithuania 57(6):535
5. Chen X et al (2022) Fullerenol protects cornea from ultraviolet B exposure. Redox Biol 54:102360
6. Mahendra CK et al (2020) Detrimental effects of UVB on retinal pigment epithelial cells and its role in age-related macular degeneration. Oxidative Med Cell Long 2020:1114
7. He J et al (2017) PTEN reduced UVB-mediated apoptosis in retinal pigment epithelium cells. Biomed Res Int 2017:1111
8. Korhonen E et al (2020) Only IL-1 beta release is inflammasome-dependent upon ultraviolet B irradiation although IL-18 is also secreted. FASEB J 34(5):6437–6448
9. Chou WW et al (2012) Tannic acid suppresses ultraviolet B-induced inflammatory signaling and complement factor B on human retinal pigment epithelial cells. Cell Immunol 273(1):79
10. Ivanov IV et al (2018) Ultraviolet radiation oxidative stress affects eye health. J Biophotonics 11(7):1145
11. An HM et al (2022) Study on the key volatile compounds and aroma quality of jasmine tea with different scenting technology. Food Chem 385:1112
12. Tang YY et al (2021) Novel antioxidant and hypoglycemic water-soluble polysaccharides from jasmine tea. Foods 10(10):123
13. Kuroda K et al (2005) Sedative effects of the jasmine tea odor and (R)-(-)-linalool, one of its major odor components, on autonomic nerve activity and mood states. Eur J Appl Physiol 95(2–3):107–114
14. Joniova J, Wagnieres G (2020) Catechin reduces phototoxic effects induced by protoporphyrin IX-based photodynamic therapy in the chick embryo chorioallantoic membrane. J Biomed Opt 25(6):1–9
15. Chen MC et al (2017) Changes in the volatiles, chemical components, and antioxidant activities of Chinese jasmine tea during the scenting processes. Int J Food Prop 20(3):681–693
16. Sharma P et al (2018) Tea polyphenols for the prevention of UVB-induced skin cancer. Photodermatol Photoimmunol Photomed 34(1):50–59
17. Kim H-M et al (2022) Theabrownin in black tea suppresses UVB-induced matrix metalloproteinase-1 expression in HaCaT keratinocytes. Biotechnol Bioprocess Eng 27(3):379–385
18. Barg M et al (2014) Evaluation of the protective effect of Ilex paraguariensis and Camellia sinensis extracts on the prevention of oxidative damage caused by ultraviolet radiation. Environ Toxicol Pharmacol 37(1):195–201
19. Davis SL et al (2022) Protection of hair from damage induced by ultraviolet irradiation using tea (Camellia sinensis) extracts. J Cosmet Dermatol 21(5):2246–2254
20. Wu QX et al (2022) Epigallocatechin gallate enhances human lens epithelial cell survival after UVB irradiation via the mitochondrial signaling pathway. Mol Med Rep. https://doi.org/10.3892/mmr.2022.12603
21. Shi J et al (2022) Updates on the chemistry, processing characteristics, and utilization of tea flavonoids in last two decades (2001–2021). Critical Rev Food Sci Nutrition 14:2568
22. Pfaffl MW (2001) A new mathematical model for relative quantification in real-time RT-PCR. Nucleic Acids Res 29(9):e45–e45
23. Wang Y et al (2022) The impact of different withering approaches on the metabolism of flavor compounds in oolong tea leaves. Foods 11(22):1114
24. Cullen AP (2011) Ozone depletion and solar ultraviolet radiation: ocular effects, a united nations environment programme perspective. Eye Contact Lens Sci Clin Pract 37(4):185–190
25. Abotorabi Z et al (2020) Jujube and green tea extracts protect human fibroblast cells against UVB-mediated photo damage and MMP-2 and MMP-9 production. Avicenna J Phytomed 10(3):287–296
26. Xu JY et al (2010) Green tea polyphenols attenuating ultraviolet B-induced damage to human retinal pigment epithelial cells in vitro. Invest Ophthalmol Vis Sci 51(12):6665–6670
27. Yin Y et al (2019) Arsenic enhances cell death and DNA damage induced by ultraviolet B exposure in mouse epidermal cells through the production of reactive oxygen species. Clin Exp Dermatol 44(5):512–519
28. Zhang D et al (2017) Echinacoside alleviates UVB irradiation-mediated skin damage via inhibition of oxidative stress, DNA damage, and apoptosis. Oxidative Med Cell Long 2017:1236
29. Cao GF et al (2012) EGCG protects against UVB-induced apoptosis via oxidative stress and the JNK1/c-Jun pathway in ARPE19 cells. Mol Med Rep 5(1):54–59
30. Musial C, Kuban-Jankowska A, Gorska-Ponikowska M (2020) Beneficial properties of green tea catechins. Int J Mol Sci 21(5):1744
31. Li YF et al (2019) Chemical compositions of chrysanthemum teas and their anti-inflammatory and antioxidant properties. Food Chem 286:8–16
32. Xu YQ, Gao Y, Granato D (2021) Effects of epigallocatechin gallate, epigallocatechin and epicatechin gallate on the chemical and cell-based antioxidant activity, sensory properties, and cytotoxicity of a catechin-free model beverage. Food Chem 339:128060
33. Liu X et al (2014) Research on synergistic protection and repairing effects of EGCG and theanine in oxidative damaged cells. J Tea Sci 34(3):239–247
34. Bhat AH et al (2015) Oxidative stress, mitochondrial dysfunction and neurodegenerative diseases; a mechanistic insight. Biomed Pharmacother 74:101–110
35. Kadenbach B, Ramzan R, Vogt S (2009) Degenerative diseases, oxidative stress and cytochrome c oxidase function. Trends Mol Med 15(4):139–147
36. Adams JM, Cory S (2018) The BCL-2 arbiters of apoptosis and their growing role as cancer targets. Cell Death Differ 25(1):27–36
37. Bock FJ, Tait SWG (2020) Mitochondria as multifaceted regulators of cell death. Nat Rev Mol Cell Biol 21(2):85–100
38. Rice M et al (2021) A role of flavonoids in cytochrome c-cardiolipin interactions. Bioorganic Med Chem 33:116043
39. Zhang J et al (2022) Complex molecular mechanism of ammonia-induced apoptosis in chicken peripheral blood lymphocytes: miR-27b-3p, heat shock proteins, immunosuppression, death receptor pathway, and mitochondrial pathway. Ecotoxicol Environ Safety 236:1123
40. Liu P et al (2021) Epigallocatechin-3-gallate protects cardiomyocytes from hypoxia-reoxygenation damage via raising autophagy related 4C expression. Bioengineered 12(2):9496–9506

41. Hsieh M-H et al (2021) Cerebral cortex apoptosis in early aged hypertension: effects of epigallocatechin-3-gallate. Front Aging Neurosci 13:1145
42. Liu M-L, Yu L-C (2008) Potential protection of green tea polyphenols against ultraviolet irradiation-induced injury on rat cortical neurons. Neurosci Lett 444(3):236–239
43. Nozza E, Rhus coriaria L et al (2020) Fruit extract prevents UV-A-induced genotoxicity and oxidative injury in human microvascular endothelial cells. Antioxidants 9(4):123
44. Cam ST et al (2015) Tea extracts protect normal lymphocytes but not leukemia cells from UV radiation-induced ROS production: An EPR spin trap study. Int J Radiat Biol 91(8):673–680

Publisher's Note